Appl Microbiol Biotechnol (2009) 81:855–863
DOI 10.1007/s00253-008-1662-4

BIOTECHNOLOGICALLY RELEVANT ENZYMES AND PROTEINS

Biochemical characterization of a novel dual-function arabinofuranosidase/xylosidase isolated from a compost starter mixture

Kurt Wagschal · Chamroeun Heng · Charles C. Lee · Dominic W. S. Wong

Received: 17 April 2008 / Revised: 24 July 2008 / Accepted: 6 August 2008 / Published online: 2 September 2008

Abstract The gene encoding a glycoside hydrolase family 43 enzyme termed deAX was isolated and subcloned from a culture seeded with a compost starter mixed bacterium population, expressed with a C-terminal His_6-tag, and purified to apparent homogeneity. deAX was monomeric in solution and had a broad pH maximum between pH 5.5 and pH 7. A twofold greater k_{cat}/K_m for the *p*-nitrophenyl derivative of α-L-arabinofuranose versus that for the isomeric substrate β-D-xylopyranose was due to an appreciably lower K_m for the arabinofuranosyl substrate. Substrate inhibition was observed for both 4-methylumbelliferryl arabinofuranoside and the xylopyranoside cogener. While no loss of activity was observed over 4 h at 40°C, the observed $t_{1/2}$ value rapidly decreased from 630 min at 49°C to 47 min at 53°C. The enzyme exhibited end-product inhibition, with a K_i for xylose of 145 mM, 18.5 mM for arabinose, and 750 mM for glucose. Regarding natural substrate specificity, deAX had arabinofuranosidase activity on sugar beet arabinan, 1,5-α-L-arabinobiose, and 1,5-α-L-arabinotriose, and wheat and rye arabinoxylan, while xylosidase activity was detected for the substrates xylobiose, xylotriose, xylotetraose, and arabinoxylan from beech and birch. Thus, deAX can be classified as a dual-function xylosidase/arabinofuranosidase with respect to both artificial and natural substrate specificity.

Keywords Arabinofuranosidase · Xylosidase · Bifunctional enzyme · Glycoside hydrolase family 43 · Compost · Hemicellulose degradation · Substrate inhibition

K. Wagschal (✉) · C. Heng · C. C. Lee · D. W. S. Wong
USDA Agricultural Research Service,
Western Regional Research Center,
800 Buchanan Street,
Albany, CA 94710, USA
e-mail: kurt.wagschal@ars.usda.gov

Introduction

Hemicelluloses (xylans, arabinoxylans) are the second most abundant carbohydrate polymer type on earth due to their being structural components in plant cell walls where they cross-link with lignin and are extensively hydrogen-bonded to cellulose (Bajpai 1997). As such, lignocellulosic biomass, composed mainly of cellulose, lignin, and hemicellulose, is seen as an underutilized feedstock that can help supply a growing demand for renewable energy resources. Structurally, xylans are heteropolysaccharides consisting of a linear β-D-(1→4)-linked xylopyranoside backbone that, depending on the tissue source, is variously substituted with arabinose and other substituents. The xylose backbone of cereal xylans can be substituted with (1→2)- and/or (1→3) linked α-L-arabinofuranosyl, α-D-glucuronic acid, and *O*-2 and/or *O*-3 linked acetate groups. Moreover, the α-L-arabinofuranose branch residues can themselves be esterified with ferulate and *p*-coumarate residues, which may in turn be cross-linked as well as be oxidatively coupled to lignin.

Numerous enzymes with the ability to hydrolyze the various hemicellulose linkages have been isolated, most of them from microbial sources (Shallom and Shoham 2003). Enzymes that hydrolyze non-reducing terminal α-L-arabinofuranosidic linkages and release arabinose in an *exo*-manner from substrates such as arabinoxylan, arabinan, and from synthetic substrates such as *p*-nitrophenyl-α-L-arabinofuranoside are classified as α-L-arabinofuranosides (AFase, EC 3.2.1.55) and are found in glycosyl hydrolase (GH) families 3, 10, 43, 51, 54, and 62. AFases are important for enzymatic biomass depolymerization since removal of the arabinose residues from the xylan backbone can have a synergistic effect with endoxylanase hydrolysis, presumably because endoxylanase hydrolysis of glycosidic bonds is inhibited by arabinose-substituted xylose residues

(Rahman et al. 2003; Sørensen et al. 2005). AFases also can act synergistically with endo-arabinases to completely depolymerize arabinans, which are one of the most abundant neutral sugar side chains of pectin in plant primary cell walls (Spagnuolo et al. 1999; Zykwinska et al. 2007). β-Xylosidases (EC 3.2.1.37) are exo-type glycosidases that catalyze the successive removal of β-xylosyl residues from the non-reducing termini of xylobiose and higher linear β-1,4-xylooligosaccharides and are found in GH families 3, 30, 39, 43, 51, 52, and 54 (Biely 2003; Shallom and Shoham 2003). In conjunction with β-xylanases which have endo-xylanolytic activity, β-xylosidases are essential in completely depolymerizing xylan. D-Xylopyranose and L-arabinofuranose are spatially similar such that the glycosidic bonds and hydroxyl groups can be overlaid, leading to bifunctional xylosidase–arabinofuranosidase enzymes (Mai et al. 2000; Lee et al. 2003; Jordan and Li 2007). Such bifunctional enzymes are of great interest since the presence of synergetic activities in the same active site may benefit industrial processes using enzymes for biomass depolymerization. We describe here the isolation of DNA from a culture seeded with a commercial compost starter and the subsequent identification, cloning with a C-terminal His_6-tag, and biochemical characterization of a bifunctional α-L-arabinofuranosidase/β-D-xylosidase termed deAX.

Materials and methods

Genomic DNA preparation Dr. Earth compost starter (Dr. Earth Company, Los Angeles, CA, USA) containing *Bacillus subtilis*, *Bacillus cereus*, *Bacillus megaterium*, *Azobacter vinelandi*, *Rhizobium japonicum*, and *Lactobacillus acidophilus* was used to inoculate a minimal media liquid culture (EZ Rich defined media; Teknova, Hollister, CA, USA) supplemented with 0.67% (*w*/*v*) each of xylan from birch wood, beech wood, and oat spelt (Sigma, St. Louis, MO, USA). The culture was grown overnight at 30°C and 200 rpm. Cells were isolated by centrifugation, and genomic DNA was isolated from the cell pellet using the FastDNA Kit (Qbiogene, Irvine, CA, USA) with Lysing Matrix 2 and CLS-TC solution according to the manufacturer's protocol.

Genomic library construction and activity screening Genomic DNA isolated from the Dr. Earth compost starter was partially digested with *Apo*I restriction enzyme. The digest was separated using agarose gel electrophoresis, and fragments 4–10 kB were excised and purified using the QiaExII gel purification kit (Qiagen, Valencia, CA, USA). These fragments were then ligated to an *Eco*RI-digested Lambda ZAP II vector and packaged into lambda phage using Lambda ZAP II Vector and Gigapack III packaging extract (Stratagene, La Jolla, CA, USA). XL1-Blue MRF' cells (Stratagene) were infected with the phage genomic DNA library and spread onto NZY (0.5% sodium chloride, 0.2% magnesium sulfate heptahydrate, 0.5% yeast extract, 1% casein hydrosylate, and 1.5% agar) media plates. The infection was overlaid with agarose containing RBB-xylan (4-*O*-methyl-D-glucurono-D-xylan-remazol brilliant blue R; Megazyme, Bray, Ireland), a soluble chromogenic substrate for the assay of endo-1,4-β-xylanases (Biely et al. 1985). Clearings in the vividly dark blue RBB-xylan overlay indicated the presence of phage plaques encoding xylan-degrading genes. The plaques were isolated and purified by repeated screenings on RBB-xylan. Single-clone excision was conducted according to the manufacturer's protocol (Stratagene) to obtain a pBS-SK construct with an inserted fragment of genomic DNA.

Subcloning of the deAX gene A cloned fragment of genomic DNA was sequenced in its entirety. An open reading frame encoding a putative GH family 43 enzyme was discovered using the VectorNTI software package (Invitrogen, Carlsbad, CA, USA) and BLAST analysis (Altschul et al. 1990). The gene was isolated by polymerase chain reaction (PCR) using Pfu DNA polymerase (Stratagene) and the following primers of which the 3′ primer contained a linker encoding the *Xho*I restriction enzyme recognition site (italicized):

deAX-5′ ATGACTAAACCATCGATAACCTATTC CAACC

deAX-3′ GCG*CTCGAG*ATTACCTCCTCTTGTC TGCCGGG

The pET-22b(+) plasmid (EMD Biosciences, San Diego, CA, USA) was digested with *Nde*I and then treated with T4 DNA polymerase (New England Biolabs) to create blunt ends. The resulting pET-22b(+) DNA and the PCR-amplified deAX gene were both digested with the *Xho*I restriction enzyme and ligated to create a pET22b(+)-deAX expression vector with the addition of the two amino acid residues LE and a C-terminal hexa-His-tag immediately following the native sequence. The deAX gene sequence has been deposited in the GenBank database under accession number EU636010.

deAX expression and purification The expression host *Escherichia coli* BL21(DE3) was transformed with the expression plasmid pET22b(+) containing the deAX insert, streaked onto Luria–Bertani agar plates amended with 50 μg/ml carbenicillin (Sigma), and incubated overnight at 37°C. Positive transformants were selected based on enzymatic hydrolysis of 4NPA (described below) and restriction digestion of the plasmids. A glycerol stock stab was used to inoculate a 100-ml seed culture of *E. coli*,

which was then grown in Terrific Broth (Research Products International) amended with 50 μg/ml carbenicillin (TB_{carb}) broth at 37°C at 250 rpm for 16 h. A 100 ml aliquot was used to inoculate 1,000 ml TB_{carb}, which was grown at 37°C to $OD_{600\ nm}$=2–3. Then the culture was cooled before inducing protein expression with 0.5 mM IPTG, and incubation was allowed to proceed at 25°C at 170 rpm overnight (~16 h). Aliquots (400–500 ml) were pelletted and the pellets stored frozen at −80°C. Cell lysis and release of soluble proteins was achieved by adding to each pellet a 65-ml solution containing 65 ml CelLytic B cell lysis reagent, 0.5 mg/ml hen egg white lysozyme, 2 mM β-mercaptoethanol (BME), 5 U/ml Benzonase (all from Sigma-Aldrich), and 1 μl/ml CalBiochem protease inhibitor cocktail III (EMD Biosciences). Cells were incubated with tube rotation on a Lab-Quake (Barnstead/Thermolyne, Dubuque, IA, USA) in the lysis solution for 30 min at room temperature, cooled to 0–4°C, and centrifuged to remove cell debris. The protein was purified using Ni-NTA resin (Qiagen) according to the manufacturer's instructions by first adjusting the supernatant solution to 300 mM NaCl, 25 mM imidazole, 2 mM BME, and 50 mM phosphate buffer (pH 8.0) before loading onto a Ni-NTA column. The composition of the wash buffer used was 50 mM phosphate buffer (pH 8.0) containing 10% glycerol, 2 mM BME, 1 μl/ml protease inhibitor cocktail III, 300 mM NaCl, and 25 mM imidazole. The protein was eluted using the same buffer except that the imidazole concentration was increased to 250 mM. Ni-NTA column fractions were analyzed by polyacrylamide gel electrophoresis (PAGE), and those containing the enzyme were pooled and purified to apparent homogeneity by size exclusion chromatography using a Superdex 200 16/60 column (GE Life Sciences) with a flow rate of 0.3 ml/min and a running buffer consisting of 50 mM phosphate buffer (pH 6.2) containing 1 mM dithiothreitol (DTT), 150 mM NaCl, and 10% glycerol. Protein concentrations were determined using Coomassie Plus reagent (Pierce Biotechnology, Rockford, IL, USA) following the manufacturer's protocol. Enzyme fractions were analyzed using PAGE following the manufacturer's protocol (Invitrogen).

Molecular weight determination The molecular weight of the His_6-tagged protein was estimated by gel filtration chromatography of a 42 μM deAX solution using Amersham Biosciences Superdex™ 200 10/300 GL and Superdex™ 75 10/300 GL columns (Amersham Biosciences) and monitoring eluant absorbance at 280 nm. The running buffer was 50 mM phosphate (pH 6.2), 150 mM NaCl, 1 mM DTT, and 10% glycerol (*w*/*v*), and a standard curve was generated with low-molecular-weight (13.7 to 67 kDa) and high-molecular-weight (158 to 669 kDa) standards (Amersham Biosciences).

Activity versus pH profile The effect of pH on the apparent V_{max} (Fig. 1) was measured using endpoint assays utilizing an equal volume of 1 M Na_2CO_3 to quench the reactions and raise all the pH values to ~pH 11. Reactions conditions were 40°C, 4 mM 4NPX, 0.1% bovine serum albumin (BSA; Sigma), 100 mM citrate for pH 3 to pH 6.5, 100 mM phosphate for pH 6.5 to pH 8.0, and 100 mM AMPSO for pH 8.0 to pH 9.5.

Enzyme assays For assays using nitrophenyl (NP) β-D-xylopyranoside and α-L-arabinofuranoside glycosides as substrates (NPX and NPA, respectively; Sigma), the enzyme activity was determined by measuring the change in absorbance at 400 nm due to NP release using a Spectramax M2 spectrophotometer equipped with a temperature controller (Molecular Devices, Sunnyvale, CA, USA). For assays using 4-methylumbelliferyl-β-D-xylopyranoside and 4-methylumbelliferyl-α-L-arabinofuranoside as substrates (muX and muA, respectively; Sigma), the enzyme activity was determined by measuring the change in fluorescence using an excitation wavelength of 349 nm and an emission wavelength of 460 nm. In a typical kinetic assay, 240 μl of 50 mM phosphate buffer (pH 6.2) containing 0.1% BSA and varying substrate concentrations was pre-incubated at 40°C for 5 min, then 10 μL enzyme solution was added and mixed to initiate the reaction. Generally, 16 different substrate concentrations, each in quadruplicate, were used to assess the kinetic parameters reported in Table 1. To accurately obtain the kinetic parameters for each substrate, the amount of enzyme was chosen so that the proportion of substrate hydrolyzed at the end of the data acquisition period generally ranged from <1% to 10%. Kinetic parameters for the hydrolysis of the natural substrates xylobiose (X2), xylotriose (X3), and xylotetraose (X4; Wako Chemicals USA, Richmond, VA, USA) were measured simultaneously on a

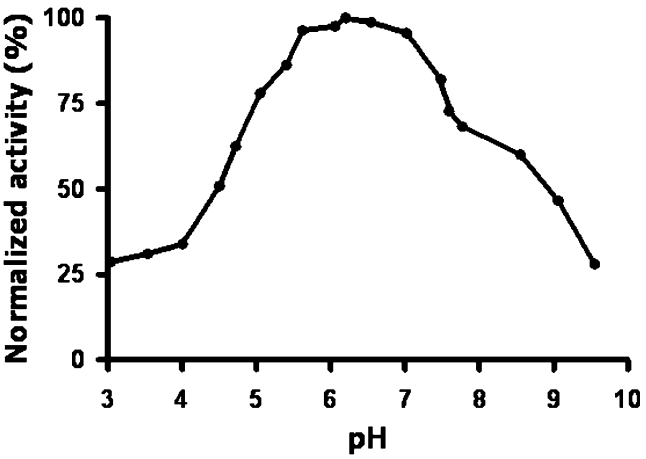

Fig. 1 Relative enzyme activity at the indicated pH values. Enzyme activity was determined with 4 mM 4NPX (*circle*). Reaction conditions were as described in "Materials and methods"

Table 1 Kinetic parameters for deAX substrate hydrolysis

Substrate[a]	Concentration range (mM)	K_m (mM)	k_{cat} (s^{-1})	k_{cat}/K_m ($mM^{-1}\cdot s^{-1}$)
4NPA[b]	0.048–3.2	0.072±0.011	0.120±0.004	1.68±0.26
4NPX[b]	0.024–9.6	1.53±0.197	1.34±0.13	0.885±0.200
2NPX[b]	0.012–20	2.03±0.240	18.7±0.7	9.2±1.1
muA[c]	0.002–1.9	0.0032±0.0004	0.035±0.001	10.8±1.3
muX[c]	0.002–7.6	0.213±0.032	1.94±0.16	8.9±1.5
X2[b]	1.25–60	15.9±1.3	0.047±0.002	0.0029±0.0003
X3[b]	1.25–80	10.4±2.0	0.044±0.003	0.0042±0.0008
X4[b]	1–20	7.5±1.8	0.019±0.002	0.0025±0.0007

[a] Reaction conditions were either 50 or 100 mM PO_4, pH 6.2, 40°C, 0.1% BSA, and deAX concentrations as described in the text.
[b] Parameters obtained from nonlinear regression fitting to the Michaelis–Menten equation
[c] Parameters obtained from nonlinear regression fitting to Eq. 1 derived from a substrate uncompetitive inhibition model. K_i (muA)=410±40 μM, K_i (muX)=1020±150 μM.

single microtitre plate in duplicate assays ([deAX]=1 μM) using a spectrophotometric enzyme-coupled assay as previously described (Wagschal et al. 2005). The kinetic parameters k_{cat} and K_m in Table 1 were calculated by nonlinear regression fitting of the data to the either the Michaelis–Menten equation using the program GraFit 5 (Erithacus Software, Surrey, UK) or to Eq. 1, derived from an uncompetitive substrate inhibition model (Malet and Planas 1997), using GraphPad Prism 4 (GraphPad Software, San Diego, CA, USA):

$$v_0 = \frac{k_{cat} \times [E_0] \times [S]}{K_m + [S] \times \left[S^2/K_i\right]}. \quad (1)$$

The inhibition constant K_i for arabinose was determined using a kinetic spectrophotometric assay wherein velocity was measured in the absence of added monosaccharide and then in the presence of 25, 50, and 100 mM arabinose using 4NPA as the substrate at concentrations ranging from 24 to 6,400 μM in a reaction buffer consisting of 50 mM PO_4 (pH 6.2), 0.1% BSA, and 240 nM deAX. The K_i for arabinose was also measured using 4NPX as the substrate using arabinose concentrations of 12.5, 25, 50, 100, and 150 mM. Arabinose at the various concentrations and deAX were pre-incubated in the assay buffer for 10 min at 40°C and the reaction initiated by adding the substrate. The K_i for xylose was obtained employing xylose concentrations of 100, 200, 300, 400, and 500 mM, 4NPX concentrations from 24 to 6400 μM, and 90 nM deAX. The K_i for glucose was similarly obtained using glucose concentrations of 500 and 2,000 mM, 4NPX concentrations from 24 to 6,400 μM, and 250 nM deAX. The K_i values were calculated by nonlinear curve fitting of the data to a competitive inhibition model using GraphPad Prism 4 (GraphPad Software).

Activity versus temperature and thermostability profiles The effect of temperature on enzyme stability (Fig. 2) was determined by first measuring the rate of 4NPX hydrolysis prior to thermal challenge. Reaction conditions were 40°C, 50 mM HPO_4 (pH 6.2), 0.1% BSA, 1 mM DTT, 4 mM 4NPX, and 160 nM deAX. Then aliquots of the enzyme solution were transferred to a 96-well PCR plate and subjected to incubation at a series of temperatures ranging from 33°C to 57°C for 20 min using a temperature gradient PCR machine (MJ Research, Watertown, MA, USA). After thermal treatment, the enzyme activity was again measured to allow calculation of the residual activity. Eight data points were obtained for each temperature tested and the residual activity calculated as a percentage of the highest recorded initial activity. The effect of temperature on the apparent V_{max} (Fig. 2) was determined by performing endpoint assays where deAX was incubated for 20 min at the various temperatures using 4 mM 4NPX substrate concentrations, quenched with an equal volume of Na_2CO_3, and *p*-NP release quantitated using a standard curve generated on the same microtiter plate.

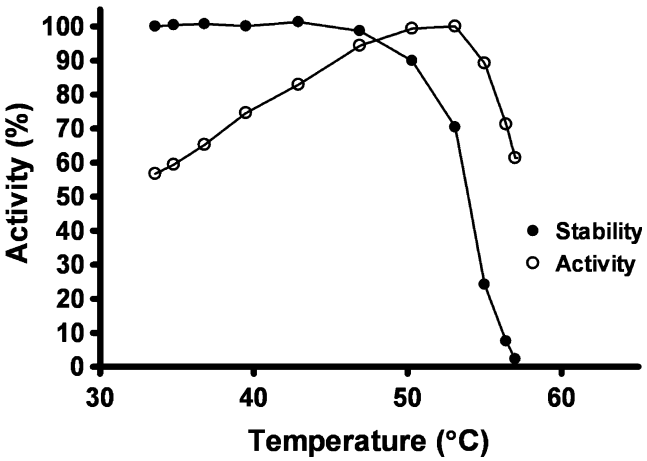

Fig. 2 Enzyme stability at the indicated temperatures (*filled circle*) and enzyme activity (relative V_{max}) at the indicated temperatures (*open circle*). Reaction conditions were as described in "Materials and methods"

Thermal inactivation half-life Aliquots (120 μL) of 1333 nM deAX in an assay buffer consisting of 50 mM phosphate, pH 6.2, 10% glycerol, and 0.1% BSA were incubated in PCR plates on an MJ Research PTC-200 thermocycler set to a given single temperature to study irreversible thermal denaturation. Aliquots were taken at specific time points and placed on ice before assaying. To assay, the enzyme was pre-incubated at 40°C for 10 min to allow refolding (Schwimmer 1944) before 6.7 mM 4NPA substrate in 150 μl assay buffer was added. Half-lives of thermal inactivation were calculated using $t_{1/2}=ln2/k_{inact}$, where k_{inact} is the inactivation rate constant obtained from the slope by plotting log (residual activity/initial activity) versus time. The reported results (Fig. 3) are the average of triplicate assays.

Substrate specificity Capillary electrophoresis (CE) was used to monitor the degradation of the following natural polymeric substrates: rye flour arabinoxylan, wheat medium viscosity arabinoxylan (all from Megazyme), birchwood xylan, and beechwood xylan (all from Sigma). Thin layer chromatography (TLC) was used to monitor the degradation of sugar beet arabinan and debranched sugar beet arabinan (Megazyme). The composition of these natural substrates as specified by the supplier and by gas–liquid chromatography (GLC) analysis are as follows. The sugar beet arabinan substrate consisted of a 1,5-α-linked arabinose backbone to which 1,3-α-linked and possibly some 1,2-α-linked L-arabinofuranosyl groups were attached. Approximately 60% of the main chain arabinofuranosyl residues were substituted by single 1,3-linked arabinofuranosyl groups. The cereal grain natural arabinoxylan substrates had homopolymeric backbones of (1-4)-β-D-xylopyranosyl residues substituted with (1-2)- and/or (1-3)-α-linked L-arabinofuranosyl branch units. The wheat arabinan medium viscosity arabinoxylan had an arabinose/xylose/other sugars ratio of 37:61:2. The rye flour arabinoxylan had a sugar composition of arabinose/xylose/other sugars of 49:48:3. The xylans from the two hardwood substrates birchwood and beechwood were each specified as containing >90% xylose residues. In-house GLC analysis of trifluoroacetic acid hydrolsylates of the beechwood and birchwood xylan used showed that each contained about 0.5% (dry weight basis) arabinose. Reaction conditions for testing hydrolysis by deAX were overnight incubation at 37°C in 115 μl of reaction buffer containing 100 mM phosphate, pH 6.5, 1 μl/ml CalBiochem protease inhibitor cocktail III, 5 mM DTT, 0.1% BSA, natural substrate concentrations between 0.9 and 2.2 mg/ml for the arabinoxylans or 20 mM for xylobiose and xylotriose, 2.9 μM deAX for the hydrolysis reactions, and no enzyme for parallel no-enzyme incubations. The samples were centrifuged and a 100 μl aliquot from each reaction lyophilized prior to derivatization. 1-Aminopyrene-3,6,8-trisulphonate (APTS) derivatization was performed by adding 6 μl 100 mM APTS in 15% acetic acid and 12 μl 1 M $NaBH_3CN$ in THF and allowing the derivatization reaction to occur overnight at 37°C. The samples were then stored at −20°C and aliquots diluted 200- to 400-fold prior to analysis by CE. Analyses were performed on a P/ACE MDQ CE system (Beckman Coulter, Fullerton, CA, USA). Separations were performed using a 20-cm uncoated fused-silica capillary column of 50-μm internal diameter (MicroSolv Technology, Long Branch, NJ, USA). Analyses were carried out at 25°C with an applied voltage of 30 kV using 50 mM phosphate, pH 7.4, as the running electrolyte. A typical run schedule was 0.5 min at 50 psi 0.1 N HCl, 0.5 min at 50 psi H_2O, 0.5 min at 50 psi 0.1 N NaOH, 0.5 min at 50 psi 1 M phosphate pH 7.4, 4 min at 80 psi 50 mM phosphate pH 7.4, conditioning at 30 kV for 5 min, injection 5 s at 0.5 psi and separation at 30 kV. The detection system was a Beckman laser-induced fluorescence detector using an excitation wavelength of 488 nm and detection at 520 nm. TLC was performed using high-performance TLC silica plates (Alltech, Waukegan, IL, USA) with mobile phase composition EtOAc/MeOH/H_2O 7:2:1. Detection was performed using 20% H_2SO_4 in MeOH with 1 mg/ml orcinol (Aldrich).

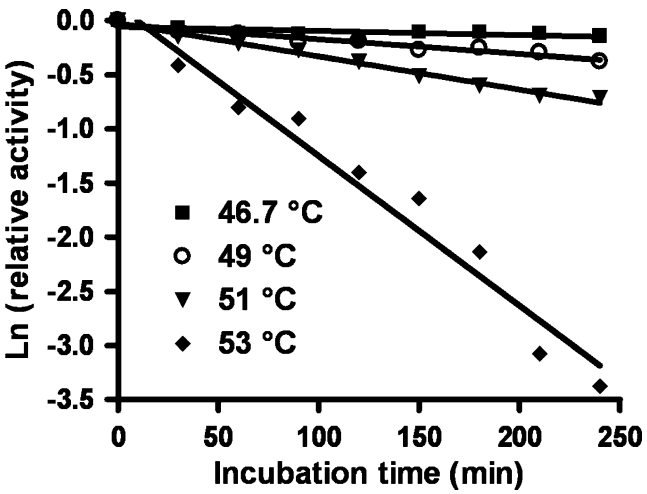

Fig. 3 Effect of temperature on the $t_{1/2}$ for thermal denaturation of deAX at the indicated temperatures. Reaction conditions were as described in "Materials and methods"

Action on the following artificial aryl-glycoside substrates was tested: *p*-NP-β-D-xylopyranoside (4NPX), *p*-NP-α-D-xylopyranoside, *o*-NP-β-D-xylopyranoside (2NPX), *p*-NP-α-L-arabinofuranoside (4NPA), *p*-NP-α-L-arabinopyranoside, *p*-NP-β-L-arabinopyranoside, *p*-NP-α-D-glucopyranoside, *p*-NP-β-D-glucopyranoside, *p*-NP-α-L-fucopyranoside, *p*-NP-β-D-fucopyranoside, *p*-NP-α-D-galactopyranoside, *p*-NP-β-D-galactopyranoside, *p*-NP-α-D-mannopyranoside, and *p*-NP-β-D-mannopyranoside (all from Sigma or Research Products International Corporation). Reaction conditions were 300 nM deAX, 4 mM aryl-

glycoside substrate, 50 mM phosphate buffer pH 6.2, 0.1% BSA and 40°C. Nitrophenyl group release was monitored by measuring the change in absorbance at 400 nm.

Results

Cloning and analysis of the deAX gene

deAX was discovered by complete sequencing of a phage plaque, derived from a mixed-population genomic DNA library, that tested positive for β-1,4-xylanase activity in an RBB-xylan zone-clearing assay. The gene encoding deAX consisted of an open reading frame of 1584 nucleotides encoding a nascent polypeptide of 527 amino acids with a predicted molecular weight of 59.1 kDa. Phylogenetic analysis of the evolutionary relationship of the amino acid sequence of deAX to other GH's places deAX in GH family 43 in the CAZY database (http://www.cazy.org/; Coutinho and Henrissat 1999), with closest relation to a β-xylosidase/α-arabinofuranosidase that is part of an aldouronate utilization gene cluster from *Paenibacillus* sp. strain JDR-2 (63% positive, 53% identical; NCBI accession ABV90487; Chow et al. 2007) and an α-arabinofuranosidase (deAFc) isolated previously from the same commercial compost starter mixture as deAX (63% positive, 50% identical; NCBI accession ABB92159; Wagschal et al. 2007). deAX is similar to a GH family 43 β-D-xylosidase XynB3 from *Geobacillus stearothermophilus* T-6 (45% positive, 34% identical; NCBI accession ABI49959) for which the catalytic active site carboxylate residues have been identified (Shallom et al. 2005). Alignment of the amino acid sequences of deAX and XynB3 reveals high homology around the active site residues, with Asp19 predicted to be the general base (aligns with Asp 15 in XynB3), Glu179 predicted to be the general acid residue (aligns with Glu187 in XynB3), while Asp 125 (aligns with Asp 128 in XynB3) is predicted to be an invariant Asp residue found in all GH family 43 enzymes where it serves to modulate the p*K*a and orientation of the general acid residue as well as contributing to substrate binding and transition state stabilization (Brüx et al. 2006).

Enzyme properties

deAX eluted in a single peak with an elution volume corresponding to a monomeric oligomerization state under the conditions employed during gel filtration chromatography, with an apparent MW of 58.6 kDa. The activity of deAX had a broad pH maximum occurring between pH 5.5 and pH 7.5 (Fig. 1). Time course studies were performed to establish that the rate of substrate hydrolysis under saturating conditions was linear with respect to time for at least 240 min at 40°C. In 20-min incubations, the enzyme was stable up to ~48°C, whereupon the activity decreased rapidly to ~25% after 20 min at 55°C (Fig. 2). The temperature maxima (T_{max}) was found to be ~55°C in 20-min endpoint assays, whereupon activity rapidly diminished due to enzyme thermal instability. Thus, the $t_{1/2}$ for thermal denaturation was calculated to be 955 min at 46.7°C, 630 min at 49°C, 234 min at 51°C, and 47 min at 53°C (Fig. 3). The kinetic parameters for hydrolysis of 4NPA, 2NPX, 4NPX, muA, muX, X2, X3, and X4 are shown in Table 1. Interestingly, 2NPX had the largest k_{cat}/K_m value due to a large k_{cat} value of ~19 s^{-1}. deAX showed substrate inhibition when 4-methylumbelliferryl was the aglycon group, and Fig. 4 shows nonlinear regression fitting of the data to Eq. 1, derived from an uncompetitive inhibition model (Malet and Planas 1997), for hydrolysis of muX (panel a) and muA (panel b; R^2=0.99 for both substrates). The K_i for muX was 1,020±150 μM and that for muA was 410±40 μM. The insets in panels a and b in Fig. 4 show biphasic Hill plots, log $v/(V_{max}-v)=h$ log[S], which corroborate this inhibition scheme where at high substrate concentrations, a second molecule of substrate is

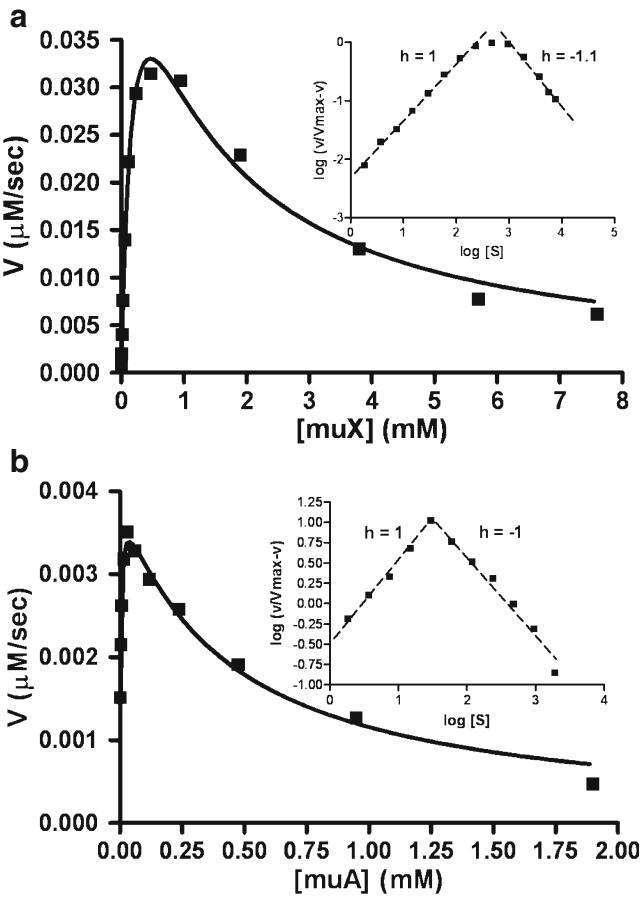

Fig. 4 Steady-state kinetics for the enzyme-catalyzed hydrolysis of muX (**a**) and muX (**b**); *insets* are Hill plots of the data. Conditions: 100 mM phosphate, pH 6.2, 0.1% BSA, 40°C, [deAX]=33.3 nM for muX and 114 nM for muA. Kinetic parameters are given in Table 1

able to bind and form an unproductive ES_2 complex, with the slope on the Hill plots then becoming −1.1 for muX and −1 for muA.

In determining synthetic substrate specificity, it was found that deAX hydrolyzed both arabinofuranosyl and xylopyranosyl synthetic aryl substrates, while no activity was detected with any of the other aryl-glycoside synthetic substrates tested (data not shown). Concerning hydrolysis of the corresponding native glycosidic bonds (Table 2), release of arabinose was observed by TLC from sugar beet arabinan, while no activity was detected on the corresponding debranched 1,5-α-linked arabinose polymer. Interestingly, deAX was also able to hydrolyze arabinobiose, releasing arabinose, as well as arabinotriose, releasing arabinose and arabinobiose. Thus, deAX appears to be able to perform hydrolysis of 1,3-α-branch points in arabinan as well as 1,5-α-linkages of shorter arabinooligosaccharides. While deAX was able to hydrolyze X2, X3, and X4, the k_{cat} values of 0.047 0.044, and 0.019 s^{-1}, respectively, were very low, and the K_m values ranged from ~8 to ~16 mM (Table 1), resulting in low catalytic efficiency factors for xylo-oligosaccharide hydrolysis. deAX released only arabinose from wheat and rye flour arabinoxylan, each of which contains ~30% arabinose. deAX released only xylose from beechwood and birchwood arabinoxylan, which contain little arabinofuranosyl substitution of the polymeric xylose backbone (Timell 1964). Based on natural and artificial substrate specificity, it can be concluded that deAX is a bifunctional α-arabinofuranosidase/β-xylosidase able to hydrolyze diverse glycosidic linkages.

Discussion

The gene encoding deAX was isolated from a positive transformant of a phage DNA library that exhibited endo-1,4-β-xylanolytic activity on the dye-labeled substrate RBB-xylan. Due to the structural complexity of xylans, where the β-1,4-xylose backbone is variously substituted with L-arabinofuranosyl, glucuronyl, 4-*O*-methylglucuronyl, and acetyl groups as well as being cross-linked through ferulate groups, the genes encoding the components of xylan degradation pathways are known to be coordinately synthesized in bacterial species (Shulami et al. 1999; Tsujibo et al. 2004). Indeed, sequence analysis of the DNA surrounding deAX indicates that it is part of an operon dedicated to hemicellulose deconstruction. Thus, in addition to the β-1,4-xylanase initially identified in the RBB-xylan clearing assay, a carbohydrate binding module was found immediately downstream of deAX, a GH family 10 xylanase was found immediately upstream of deAX, and a sequence encoding an α-glucuronidase was found 116 bp upstream of the xylanase gene.

Table 2 Survey of deAX natural substrate hydrolysis

Substrate	Monosaccharide released
Xylobiose	Xylose
Xylotriose	Xylose
Xylotetraose	Xylose
Arabinobiose	Arabinose
Arabinotriose	Arabinose
Sugar beet arabinan	Arabinose
Debranched sugar beet arabinan	None detected
Wheat arabinoxylan	Arabinose
Rye flour arabinoxylan	Arabinose
Beechwood arabinoxylan	Xylose
Birchwood arabinoxylan	Xylose

Hydrolysis reaction conditions and monosaccharide analysis as described in the text

The protein deAX eluted as a single peak during gel filtration chromatography. The apparent MW value of 58.6 kDa was within experimental error of the calculated subunit MW of 59.1 kDa; thus, the protein elutes as a monomer under the gel filtration conditions employed. Other GH 43 enzymes have been reported to have monomeric (Wagschal et al. 2007) and tetrameric (Jordan et al. 2007a) quaternary structures.

While the K_m values for 4NPX and 2NPX were similar (1.53 and 2.03 mM, respectively), the ratio k_{cat}2NPX/k_{cat}4NPX was ~14. The p*K*as of *o*-NP and *p*-NP are nearly identical (7.22 and 7.18, respectively); thus, the rate differences are not due to p*K*a differences of the leaving groups. Contributing significantly to the differences in hydrolysis rates are likely differences in non-covalent interactions of these stereo-electronically different leaving groups in the active site. While k_{cat}4NPA/k_{cat}4NPX was 0.09, K_m4NPX/K_m4NPA was ~20, with the result that the enzyme has a twofold greater catalytic efficiency factor k_{cat}/K_m for 4NPA than for 4NPX. Similar to the result obtained for 4NPA and 4NPX, k_{cat}muA/muX=0.02, while K_m was found to be significantly lower for the arabinofuranosyl substrate; K_m muX/muA=67. However, due to an extremely low K_m value for muA (~3 μM), the substrate conversion was as high as 20% for one of the lower substrate concentrations tested, and the apparent K_m value obtained thus likely represents an upper limit. deAX showed substrate inhibition with both muA and muX, with a K_i of 410 μM for muA and 1020 μM for muX, suggesting tighter binding of the arabinofuranosyl moiety than for the xylopyranosyl moiety.

It is important to assess the inhibitory binding of arabinose, xylose, and glucose to deAX since these sugars can reach concentrations of 0.3–3 M during saccharification of biomass. Thus, although none of the sugars was particularly inhibitory, with K_i values of 18.5±2.0 mM for

arabinose, 145±6 mM for xylose, and 750±130 mM for glucose, it is likely desirable to improve the tolerance of deAX to monosaccharide inhibition for use in biomass deconstruction processes. The K_i for arabinose for the arabinofuranosidase deAFc isolated from the same compost starter mixture was 27 mM (Wagschal et al. 2007), similar to that obtained for deAX. The K_i for arabinose for a catalytically efficient GH 43 enzyme isolated from *Selenomonas ruminantium* was on the order of 50–60 mM (Jordan and Braker 2007) and thus also quite similar. The K_i of deAX for xylose is at least eightfold higher than that for arabinose, indicating a less favorable environment for binding of the xylopyranosyl ring in the active site, reflected in the relatively higher K_i for muX versus that for muA and the higher K_ms for 4NPX and muX versus those for their corresponding arabinofuranosyl isomers (Table 1).

deAX hydrolyzed both arabinofuranosyl and xylopyranosyl synthetic aryl substrates, while no activity was detected with any of the other aryl-glycoside synthetic substrates (data not shown). D-Xylopyranose and L-arabinofuranose are spatially similar, thereby rationalizing the existence of bifunctional α-L-arabinofuranosidases/β-D-xylosidases with respect to synthetic substrate hydrolysis. The natural substrate specificity of deAX (Table 2) is markedly broader than that of the other GH 43 enzyme deAFc isolated from the same compost starter mixture, which was found to release only arabinose from natural substrates (Wagschal et al. 2007). Unlike deAFc, deAX was able to hydrolyze the natural substrates X2, X3, and X4, albeit with low k_{cat} and k_{cat}/K_m kinetic parameters (Table 1). This can be contrasted with the k_{cat} and k_{cat}/K_m values reported for the GH43 xylosidase SXA for hydrolysis of X2 (412 s^{-1}, 99 $mM^{-1}{\cdot}s^{-1}$), X3 (172 s^{-1}, 45 $mM^{-1}{\cdot}s^{-1}$), and X4 (150 s^{-1}, 38 $mM^{-1}{\cdot}s^{-1}$; Jordan et al. 2007b). The β-D-xylosidase from *B. pumilus* also has markedly higher reported k_{cat} and k_{cat}/K_m values for X2 (18 s^{-1}, 6.2 $mM^{-1}{\cdot}s^{-}1$), X3 (3.0 s^{-1}, 2.7 $mM^{-1}{\cdot}s^{-1}$), and X4 (3.0 s^{-1}, 2.1 $mM^{-1}{\cdot}s^{-1}$) hydrolysis (Van Doorslaer et al. 1985). deAX released arabinose from sugar beet arabinan, but not from debranched arabinan substrate, indicating specificity for 1,3-α-branch points, and was also able to release arabinose from arabinobiose and arabinotriose, consistent with an *exo*-activity for arabinan hydrolysis. deAX released only arabinose from wheat and rye arabinoxylan, while only xylose was released from either beechwood or birch arabinoxylan, both of which have very little arabinose content.

In summary, deAX displays both xylosidase and arabinofuranosidase activity on synthetic α-L-arabinofuranosides and β-D-xylopyranosides, debranching and exo-arabinofuranosidase activity on arabinan, short arabinooligosaccharides, and arabinoxylan from wheat and rye, while also displaying xylosidase activity on xylooligosaccharides and arabinoxylan from birch and beechwood.

Acknowledgments The authors would like to thank Gregory Gray for GLC analysis. Reference to a company and/or products is for purposes of information and does not imply approval or recommendation of the product to the exclusion of others which may also be suitable. All programs and services of the US Department of Agriculture are offered on a non-discriminatory basis without regard to race, color, national origin, religion, sex, age, marital status, or handicap.

References

Altschul SF, Gish W, Miller W, Myers EW, Lipman DJ (1990) Basic local alignment search tool. J Mol Biol 215:403–410

Bajpai P (1997) Microbial xylanolytic enzyme system: properties and applications. Adv Appl Microbiol 43:141–195

Biely P (2003) Xylanolytic enzymes. In: Whitaker JR, Voragen AGJ, Wong DWS (eds) Handbook of food enzymology. Marcel Dekker, New York, NY, pp 879–915

Biely P, Mislovièová D, Toman R (1985) Soluble chromogenic substrates for the assay of endo-1,4-β-xylanases and endo-1,4-β-glucanases. Anal Biochem 144:142–146

Brüx C, Ben-David A, Shallom-Shezifi D, Leon M, Niefind K, Shoham G, Shoham Y, Schomburg D (2006) The structure of an inverting GH43 β-Xylosidase from *Geobacillus stearothermophilus* with its substrate reveals the role of the three catalytic residues. J Mol Biol 359:97–109

Chow V, Nong G, Preston JF (2007) Structure, function, and regulation of the aldouronate utilization gene cluster from *Paenibacillus* sp. strain JDR-2. J Bacteriol 189:8863–8870

Coutinho PM, Henrissat B (1999) Carbohydrate-active enzymes: an integrated database approach. Cambridge, The Royal Society of Chemistry, Cambridge

Jordan DB, Braker JD (2007) Inhibition of the two-subsite β-D-xylosidase from *Selenomonas ruminantium* by sugars: competitive, noncompetitive, double binding, and slow binding modes. Arch Biochem Biophys 465:231–246

Jordan DB, Li X-L (2007) Variation in relative substrate specificity of bifunctional β-D-xylosidase/α-L-arabinofuranosidase by single-site mutations: roles of substrate distortion and recognition. Biochim Biophys Acta 1774:1192–1198

Jordan DB, Li X-L, Dunlap CA, Whitehead TR, Cotta MA (2007a) β-D-Xylosidase from *Selenomonas ruminantium* of glycoside hydrolase family 43. Appl Biochem Biotechnol 136–140:93–104

Jordan DB, Li X-L, Dunlap CA, Whitehead TR, Cotta MA (2007b) Structure–function relationships of a catalytically efficient β-D-xylosidase. Appl Biochem Biotechnol 141:51–76

Lee RC, Hrmova M, Burton RA, Lahnstein J, Fincher GB (2003) Bifunctional family 3 glycoside hydrolase from barley with α-L-arabinofuranosidase and β-D-xylosidase activity. J Biol Chem 278:5377–5387

Mai V, Wiegel J, Lorenz WW (2000) Cloning, sequencing, and characterization of the bifunctional xylosidase–arabinosidase from the thermophile *Thermoanaerobacter ethanolicus*. Gene 247:137–143

Malet C, Planas A (1997) Mechanism of *Bacillus* 1,3-1,4-β-D-glucan 4-glucanohydrolase: kinetics and pH studies with 4-methylumbelliferyl β-D-glucan oligosaccharides. Biochemistry 36:13838–13848

Rahman AKMS, Sugitani N, Hatsu M, Takamizawa K (2003) A role of xylanase, α-L-arabinofuranosidase, and xylosidase in xylan degradation. Can J Microbiol 49:58–64

Schwimmer S (1944) Regeneration of heat-inactivated peroxidase. J Biol Chem 154:487–495

Shallom D, Shoham Y (2003) Microbial hemicellulases. Curr Opin Microbiology 6:219–228

Shallom D, Leon M, Bravman T, Ben-David A, Zaide G, Belakhov V, Shoham G, Schomburg D, Baasov T, Shoham Y (2005) Biochemical characterization and identification of the catalytic residues of a family 43 β-D-Xylosidase from *Geobacillus stearothermophilus* T-6. Biochemistry 44:387–397

Shulami S, Gat O, Sonenshein AL, Shoham Y (1999) The glucuronic acid utilization gene cluster from *Bacillus stearothermophilus* T-6. J Bacteriol 181(12):3695–3704

Sørensen HR, Pedersen S, Viksø-Nielsen A, Meyer AS (2005) Efficiencies of designed enzyme combinations in releasing arabinose and xylose from wheat arabinoxylan in an industrial ethanol fermentation residue. Enzyme Microb Technol 36:773–784

Spagnuolo M, Crecchio C, Pizzigallo MDR, Ruggiero P (1999) Fractionation of sugar beet pulp into pectin, cellulose, and arabinose by arabinases combined with ultrafiltration. Biotechnol Bioeng 64:685–691

Timell T (1964) Wood hemicelluloses: part I. Adv Carbohydr Chem Biochem 19:247–299

Tsujibo H, Kosaka M, Ikenishi S, Sato T, Katsushiro M, Inamori Y (2004) Molecular characterization of a high-affinity xylobiose transporter of *Streptomyces thermoviolaceus* OPC-520 and its transcriptional regulation. J Bacteriol 186(4):1029–1037

Van Doorslaer E, Kersters-Hilderson H, De Bruyne CK (1985) Hydrolysis of β-D-xylo-oligosaccharides by β-D-xylosidase from *Bacillus pumilus*. Carbohydr Res 140:342–346

Wagschal K, Franqui-Espiet D, Lee CC, Robertson GH, Wong DWS (2005) Enzyme-coupled assay for β-xylosidase hydrolysis of natural substrates. Appl Environ Microbiol 71(9):5318–5323

Wagschal K, Franqui-Espiet D, Lee CC, Kibblewhite-Accinelli RE, Robertson GH, Wong DWS (2007) Genetic and biochemical characterization of an α-L-arabinofuranosidase isolated from a compost starter mixture. Enzyme Microb Technol 40:747–753

Zykwinska A, Thibault J-F, Ralet M-C (2007) Organization of pectic arabinan and galactan side chains in association with cellulose microfibrils in primary cell walls and related models envisaged. J Exp Bot 58:1795–1802